HHS Public Access

Author manuscript

Diabetes Obes Metab. Author manuscript; available in PMC 2019 November 01.

Published in final edited form as:

Diabetes Obes Metab. 2018 November ; 20(11): 2574–2584. doi:10.1111/dom.13423.

High Fat Diet induced Remission of Diabetes in a subset of K_{ATP}-GOF Insulin Secretory-Deficient mice

Zihan Yan[1], **Zeenat A. Shyr**[1], **Manuela Fortunato**[1], **Alecia Welscher**[1], **Mariana Alisio**[1], **Michael Martino**[2], **Brian N. Finck**[2], **Hannah Conway**[1], and **Maria S. Remedi**[1,*]

[1]Department of Medicine, Division of Endocrinology, Metabolism and Lipid Research, Washington University School of Medicine, 660 South Euclid Avenue, St. Louis, Missouri 63110, USA

[2]Department of Medicine, Division of Geriatrics and Nutritional Science, Washington University School of Medicine, 660 South Euclid Avenue, St. Louis, Missouri 63110, USA

Abstract

Chronic hyperglycemia has been proposed to cause pancreatic β-cell dysfunction and loss of β-cell mass. As in human monogenic neonatal diabetes, mice expressing K_{ATP} channel gain-of-function (GOF) mutations demonstrate deficiency in insulin secretion and develop severe diabetes. As diabetes progresses, they show loss of islet insulin content and β-cell mass, secondary consequences of glucotoxicity. Co-morbidity of chronic hyperglycemia and elevated lipids, so called glucolipotoxicity, is also crucial in the pathogenesis of diabetes. To test the effects of high-fat-diet (HFD) on neonatal diabetes, without the confounding effects of compensatory hyperinsulinemia, K_{ATP}-GOF mice were fed HFD. Surprisingly, K_{ATP}-GOF mice demonstrate resistance to HFD-induced obesity, accompanied by a markedly divergent blood-glucose control with some K_{ATP}-GOF animals showing persistent diabetes (non-remitters, K_{ATP}-GOF-NR) and others demonstrating remission of diabetes (K_{ATP}-GOF-R). Compared to the severely diabetic and insulin resistant K_{ATP}-GOF-NR mice, HFD fed K_{ATP}-GOF-R mice demonstrate lower blood glucose, improved insulin sensitivity, and increased circulating plasma insulin and GLP1 concentrations. Strikingly, while HFD fed K_{ATP}-GOF-NR mice show increased food-intake and decreased physical activity, reduced whole body fat mass and increased plasma lipids; K_{ATP}-GOF-R mice demonstrate similar features as control littermates. Importantly, K_{ATP}-GOF-R mice have restored insulin content and β-cell mass compared to the marked loss observed in both HFD K_{ATP}-GOF-NR and chow fed K_{ATP}-GOF mice. Together, our results suggest that restriction of dietary carbohydrates and caloric replacement by fat can induce metabolic changes that are beneficial in reducing glucotoxicity and secondary consequences of diabetes in a mouse model of insulin secretory-deficiency.

*Address all correspondence and reprint requests to MSR: Ph: (314) 362-6636, mremedi@wustl.edu.

AUTHOR CONTRIBUTIONS

Z.Y. and M.S.R. designed the study. Z.Y., Z.A.S, M.F., A.W., M.A., H.C., M.M. and M.S.R. performed the experiments. Z.Y and M.S.R wrote the manuscript. All authors read the manuscript and provide comments. M.S.R., Z.A.S.and B.N.F. reviewed and edited the manuscript.

The authors have no competing financial interests to declare.

INTRODUCTION

Diabetes is a major and growing public health problem, and over the past two decades obesity has substantially risen worldwide. Type-2 diabetes occurs when insulin secreting β-cells fail to adequately respond to the increased demand in the presence of insulin resistance[1,2]. In both humans and experimental animals, obesity is a leading pathogenic factor for developing insulin resistance and diabetes[3]. In animal models, β-cell failure can be accelerated or delayed by dietary modifications, therefore understanding the *in vivo* contribution of high glucose (glucotoxicity) and lipids (lipotoxicity) to β-cell failure is crucial. Many studies have demonstrated that high-fat-diet (HFD) accelerates diabetes, supporting the concept of lipotoxicity and development of insulin resistance. However, the diabetogenic effect of reduced insulin sensitivity versus the glucotoxic effect of hyperglycemia cannot entirely be ruled out. While several mouse models of diabetes have been used to study the contribution of HFD and obesity, the role of HFD in insulin secretory-deficient monogenic diabetes remains elusive.

Gain-of-function (GOF) mutations in the ATP-sensitive K^+ (K_{ATP}) channel have been identified as the main cause of human neonatal diabetes (NDM)[4] due to the inability of β-cells to secrete insulin[5]. We previously generated a mouse model of human NDM by introducing a K_{ATP}-GOF mutation into the rosa26 locus under the Cre recombinase control[6]. As expected, and mimicking the human disease, mice expressing the K_{ATP}-GOF mutation specifically in pancreatic β-cells do not secrete insulin in response to glucose and rapidly develop severe diabetes[6]. These mice show normal islet architecture in early stages of diabetes. However, as diabetes progress, they demonstrate a marked loss of islet insulin content and β-cell mass[6,7] which are classic findings in other forms of diabetes as well[8–10]. Critically, we have demonstrated that loss of β-cell mass in these mice is not due to β-cell death as frequently assumed, but instead due to loss of β-cell identity[7].

Co-morbidity of hyperglycemia and elevated free-fatty-acids (glucolipotoxicity) is also critical in the pathogenesis of diabetes[11], however little is known about the underlying mechanisms at the level of β-cell ion channel, electrical activity, Ca^{2+} homeostasis and exocytosis. To test the contribution of elevated lipids in insulin secretory deficient monogenic diabetes, K_{ATP}-GOF mice were exposed to high-fat-diet (HFD). Surprisingly, K_{ATP}-GOF mice demonstrate resistance to HFD-induced obesity and show markedly divergent blood glucose control with some K_{ATP}-GOF animals demonstrating persistent severe diabetes and others, remission of diabetes. In remitting mice, islet insulin content and β-cell mass is maintained, and remission is preceded by improved insulin sensitivity and increased circulating plasma insulin and GLP1. Together, these results demonstrate that restriction of dietary carbohydrates and caloric replacement by fat induces metabolic changes at the cellular and whole-body level that are beneficial in terms of decreasing glucotoxicity in insulin secretory-deficient diabetes.

MATERIALS AND METHODS

Animals and diets.

Animal studies were done in accordance with protocols approved by the Washington University Animal Care Committee. Animals were housed under usual 12h daylight/12h darkness circadian-clock. Tamoxifen inducible β-cell specific K_{ATP}-GOF transgenic mice were previously generated[6]. Tamoxifen (50 μg/gBW) was given for five-days to 9–10 week-old mice to promote transgene expression[6]. Single-transgenic, Pdx-Cre^{ER}TM or Rosa26-Kir6.2[K185Q,ΔN30], and wild-type littermates were used as controls[6]. To test the effect of a HFD, K_{ATP}-GOF and control littermate mice were randomly divided in two groups: 1) fed with normal chow-diet (ChD) and 2) fed with HFD initiated at the same time as tamoxifen. Four independent batches of HFD (HFD; 45% fat, Tekland-Harland) were used throughout the experiments. Blood glucose was measured in tail vein samples using a Contour blood glucose meter (Bayer Corp).

Glucose tolerance tests (GTTs) and Insulin tolerance tests (ITTs).

Blood glucose was measured in tail vein samples before (time 0) and followed by an intraperitoneal (ip) injection of 1.5 g dextrose /kg body-weight (GTT) after overnight-fast, or 0.5 U human insulin/kg body-weight (ITT, HI-210 Lilly) after five-hour fast at 15, 30, 60, 90 and 120 min post-injection, as previously described[12].

Plasma hormone measurements

Blood samples were taken from the tail vein at 22 and 110 days post-tamoxifen induction for measurement of plasma hormones. Blood was collected in heparinized tubes with protease inhibitor cocktail (3.6mg/Ml benzamidine-hydrocholoride, 1mg/mL aprotinin, 1mM Sitagliptin and 25mM EDTA). Plasma hormones were measured using Luminex-Milliplex Mouse Metabolic-Hormone panel at Vanderbilt Hormone Assay Core (http://hormone.mc.vanderbilt.edu/), and plasma lipids at Washington University Diabetes Models Phenotyping Core, (http://diabetesresearchcenter.dom.wustl.edu/diabetes-models-phenotyping-core/). CV values: Insulin: 7.2%, glucagon: 5.6%, GLP1: 11.3% and Leptin: 10.6%.

Body composition analysis using DEXA and MRI.

A validated mouse DEXA instrument (Lunar PIXImus2 Densitometer; GE Medical-Systems) at Washington University Diabetes Phenotyping Core was used to measure bone mass density (BMD; amount of minerals within bone) and percentage of fat (whole-body) in anesthetized animals[12]. Whole body DEXA analysis for BMD and percentage of body fat was performed by using a software provided by the instrument (inter-assay CV; 0.65%). A magnetic resonance imaging EchoMRI Instrument (Echo Medical Systems, Houston, TX) at Washington University Diabetes Phenotyping Core was used for defining the percentage body fat and lean mass in awake animals.

Metabolic Profile.

Comprehensive metabolic, behavioral, and physiological variables were determined by TSE/PhenoMaster at Washington University Diabetes Models Phenotyping Core to measure oxygen (O_2) consumption, carbon dioxide (CO_2) generation, physical activity and food intake. Food intake was considered as the amount of food consumed per gram of mouse lean body mass/12 hours. The respiratory exchange ratio (RER) was calculated as the ratio between the amount of CO_2 produced in metabolism and the O_2 used. Metabolic efficiency was calculated as the ratio between body weight and food consumption.

Hematoxylin-Eosin staining and Immunohistochemistry.

HFD fed mice were sacrificed 130 days after tamoxifen. Pancreases were fixed and paraffin-embedded for sectioning. Serial sections of 5μm and Hematoxylin-Eosin (H&E) staining was carried out at the Anatomic/Molecular Pathology Core, Washington University. Immunohistochemistry was carried out as previously described[7], stained with guinea pig anti-insulin (Abcam, 1:100) and mouse anti-glucagon (Cell-signaling, 1:100) antibodies, and their distribution visualized using goat anti-guinea-pig antibody conjugated with AlexaTM 488 or goat anti-mouse antibody conjugated with AlexaTM 594 (Molecular Probes, Eugene-OR), respectively, using an EXC-500 fluorescence microscope (VisualDynamix, Chesterfield, MO).

Pancreatic islet isolation, total insulin content and glucose stimulated insulin secretion

Islet isolation was performed as previously described[6]. All visible islets were manually handpicked using a dissecting microscope, and maintained overnight in CMRL-1066 (5.6mM glucose) medium (GIBCO) supplemented with 10% fetal calf serum, 100U/ml penicillin and 100μg/ml streptomycin[7]. Total insulin was extracted from islets in 0.2N/85% acid-ethanol and measured using a rat/mouse insulin Elisa-kit (Crystal-Chem, IL). Islets (10 per well) were pre-incubated in glucose-free CMRL-1066 plus 3mM glucose for 1 hour, and then incubated at 37°C in CMRL-1066 plus 3 or 23mM glucose, or 30mM KCl for one hour. Medium was then removed and insulin release was measured using Rat Insulin-radioimmunoassay (Millipore, St. Charles, MO).

Glycogen Content

Frozen liver samples (30–90mg) were hydrolyzed in 30% w/v KOH in a boiling bath for 30min. After cooling, 0.1ml 1M Na_2SO_4 and 0.8ml ethanol were added, boiled 5min and centrifuged at 10,000G/5min. The glycogen pellet was dissolved in 0.2ml water with two additional ethanol precipitations. The pellet was dried and dissolved in 0.2ml of 0.3mg/ml amyloglucosidase in 0.2M sodium-acetate buffer (pH 4.8), and incubated for 3hs at 40°C. The reaction mixture was diluted two- to five-fold in water. To determine glucose concentration, 5ml of sample was added to 0.2ml of glucose assay solution containing 0.3M triethanolamine–KOH (pH 7.5), 1mM ATP, 0.9mM b-NADP, and 5mg G-6P dehydrogenase/ml. The absorbance at 340nm was determined before and after addition of 1mg hexokinase. Glycogen content is expressed as micromoles of glucosyl units/gram wet-weight.

Statistical methods.

Data are presented as mean ± SEM. Differences between two groups were tested using t-test and among several groups were tested using analysis of variance (ANOVA) and post-hoc Turkey's test, assuming that the data is normally distributed for each variable. Significant differences among groups with *p<0.05, **p<0.01; ***p<0.001 and ****p<0.0001 are indicated, and non-significant differences are not shown.

RESULTS

Resistance to HFD-induced obesity, and remission of diabetes in K_{ATP}-GOF mice.

Upon tamoxifen injection, β-cell specific K_{ATP}-GOF mice [6]demonstrate a marked increase in blood glucose levels and become severely diabetic (Fig. 1A)[6,13]. As diabetes progresses, K_{ATP}-GOF mice show a marked decrease in islet insulin content and β-cell mass, secondary consequences of chronic hyperglycemia (glucotoxicity). To test the contribution of lipids in addition to chronic hyperglycemia (glucolipotixicity), insulin secretory-deficient K_{ATP}-GOF mice were exposed to HFD. As expected, K_{ATP}-GOF mice show increased blood glucose due to the inability to secrete insulin in response to glucose; however, they progress to a markedly divergent phenotype over time. While some HFD fed K_{ATP}-GOF mice develop severe diabetes (non-remitter, K_{ATP}-GOF-NR: 80% males and 57.14% females), others show remission of diabetes (remitter, K_{ATP}-GOF-R: 20% males and 42.86% females) (Fig. 1B). Importantly, K_{ATP}-GOF remitting and non-remitting mice appear within the same cohorts and also among K_{ATP}-GOF littermates. K_{ATP}-GOF mice fed ChD show a slight decrease in body weight over time compared to control mice (Fig. 1C). As expected, HFD fed control mice show increased body weight over time. Surprisingly, HFD fed K_{ATP}-GOF mice did not show weight gain (Fig. 1D) and they have similar weights as ChD fed K_{ATP}-GOF mice. Although all HFD fed control mice demonstrate a marked increase in body weight, males were significantly heavier than female mice but these sex differences were not present in K_{ATP}-GOF mice.

Improved insulin sensitivity in K_{ATP}-GOF-R mice precedes the lowering of blood glucose and diabetes remission on the HFD.

In addition to diabetes remission, K_{ATP}-GOF-R mice show reduced fasting blood glucose and improved glucose tolerance at 100 days post-tamoxifen compared to K_{ATP}-GOF-NR mice (Fig. 2A,B). Moreover, K_{ATP}-GOF-R mice show a marked improvement in insulin sensitivity at day 21 of HFD feeding, compared to the insulin resistant K_{ATP}-GOF-NR mice (Fig. 2C). It is important to note that the improvement in insulin sensitivity precedes the lowering of blood glucose in K_{ATP}-GOF-R mice, and it is maintained over a period of 120 days (Fig. 2D).

Increased plasma insulin and GLP1 concentrations in HFD fed K_{ATP}-GOF-R mice.

As previously demonstrated[6], ChD fed K_{ATP}-GOF mice show a marked (80%) reduction in plasma insulin compared to control littermates. However, HFD fed K_{ATP}-GOF mice show a different pattern. Circulating plasma insulin is reduced in both K_{ATP}-GOF-NR and K_{ATP}-GOF-R mice at 22 days. However, at 110 days, HFD fed K_{ATP}-GOF-R mice show an

increase in plasma insulin comparable to control mice, while it is reduced over time in K_{ATP}-GOF-NR mice (Table 1). Plasma glucagon concentration show a transient increase only in HFD fed K_{ATP}-GOF-R mice at 22 days, values that decrease to normal control levels at 110 days (Table 1). At day 22, there are no significant differences in leptin or GLP-1 concentrations in controls, K_{ATP}-GOF-NR or K_{ATP}-GOF-R mice. At 110 days, leptin is significantly decreased in both K_{ATP}-GOF-NR and K_{ATP}-GOF-R, and GLP-1 is markedly increased only in HFD fed K_{ATP}-GOF-R (Table 1).

HFD prevents loss of whole body fat mass and bone marrow density in K_{ATP}-GOF-R mice.

ChD fed K_{ATP}-GOF diabetic mice demonstrate a marked reduction in body fat mass (18.24%) compared to control littermates (27.37%), and severe bone abnormalities, including scoliosis (Fig. 3A). HFD fed K_{ATP}-GOF-NR mice have similar loss of fat and bone mass as ChD fed K_{ATP}-GOF mice but strikingly, K_{ATP}-GOF-R maintain similar body composition as HFD fed control mice (Fig. 3B). Correlating with this, MRI experiments demonstrate a marked reduction in whole body fat mass in K_{ATP}-GOF-NR diabetic mice, but not in K_{ATP}-GOF-R mice (Fig. 3C). It is important to note that whole body lean mass is similar between the three groups (Fig. 3C).

Plasma triglyceride, cholesterol and free-fatty acids concentrations are markedly increased in HFD fed K_{ATP}-GOF-NR mice but decreased to HFD fed control levels in in K_{ATP}-GOF-R mice (Fig. 3D).

Food intake is significantly increased and physical activity markedly impaired in K_{ATP}-GOF-NR mice, but is normal in K_{ATP}-GOF-R mice.

Mice fed with both ChD and HFD for 135 days were subjected to metabolic cage measurements for 72 hours. There are no significant differences in food intake or physical activity between ChD fed control and ChD fed K_{ATP}-GOF mice during the day (6AM to 6PM); however, at night (6PM to 6AM) K_{ATP}-GOF mice show significantly lower activity than control mice and no significant difference in food intake (Fig. 4A,B). Importantly, HFD fed K_{ATP}-GOF-NR diabetic mice demonstrate a significant increase in food intake and a marked decrease in movement compared to both HFD fed control and K_{ATP}-GOF-R mice at night time (Fig. 4E,F). Respiratory exchange rate (RER) is not significantly different between groups within the same diet (Fig. 4C,G); however, metabolic efficiency is markedly decreased in both ChD fed K_{ATP}-GOF (Fig. 4D) and HFD fed K_{ATP}-GOF-NR diabetic mice (Fig. 4H). There is a slight improvement in metabolic efficiency in K_{ATP}-GOF-R mice compared to control mice in the same diet group (Fig. 4H).

Avoidance of secondary loss of insulin content and β-cell mass in HFD fed K_{ATP}-GOF-R mice.

Since ChD fed K_{ATP}-GOF diabetic mice demonstrated a marked decrease in insulin content and β-cell mass[6], we tested the potential effects of HFD on pancreatic insulin content. While HFD fed K_{ATP}-GOF-NR mice show similar loss of insulin immunostaining as ChD fed K_{ATP}-GOF diabetic mice, HFD fed K_{ATP}-GOF-R mice demonstrate maintenance of insulin/glucagon immunostaining (Fig. 5A). These results correlate nicely with the total insulin content measurements in isolated islets. While total islet insulin content is markedly reduced

in HFD fed K_{ATP}-GOF-NR mice, it is partially preserved in HFD fed K_{ATP}-GOF-R (Fig. 5B). As predicted by the mutation, glucose-stimulated insulin secretion is markedly reduced in islets from both HFD fed K_{ATP}-GOF-R and K_{ATP}-GOF-NR mice compared to control islets. Insulin secretion in response to KCl depolarization is significantly reduced in islets from both K_{ATP}-GOF-R and K_{ATP}-GOF-NR compared to controls (Fig. 5C). However, K_{ATP}-GOF-R islets secrete more insulin than K_{ATP}-GOF-NR, presumably because of the marked decreased in insulin content observed in these islets (Fig. 5B). Strikingly, basal insulin secretion is significantly increased in K_{ATP}-GOF-R islets (Fig. 5C), but not in K_{ATP}-GOF-NR islets, which is consistent with the elevated plasma insulin demonstrated only in remitter mice (Table 1). Total liver glycogen content is markedly reduced in HFD fed K_{ATP}-GOF-NR mice but is normal in K_{ATP}-GOF-R mice (Figure 5D).

DISCUSSION

Is hyperinsulinemia and insulin resistance necessary for HFD-induced obesity?

Progressive deterioration of glucose homeostasis, along with loss of β-cell function and mass are classic findings in several forms of diabetes[14–16]. [1,2]Co-morbidity of hyperglycemia and elevated lipids, known as glucolipotoxicity, is also a critical factor in the development of diabetes[11]. However, it is unclear whether altered insulin secretion, hyperinsulinemia or insulin resistance have significant causal roles in the progression to type-2 diabetes[17]. We have previously demonstrated development of diabetes an insulin secretory-deficient K_{ATP}-GOF mouse model of human neonatal diabetes. K_{ATP}-GOF mice show a marked loss of insulin content and β-cell mass with the progression of diabetes. These features can be prevented or reverted by lowering blood glucose with either sulfonylureas or insulin therapy[6,7,13].

Here we show that feeding HFD to K_{ATP}-GOF mice leads to a markedly divergent blood glucose control with some animals showing persistent severe diabetes (K_{ATP}-GOF-NR) and others, remission of diabetes (K_{ATP}-GOF-R). Remission of diabetes in HFD fed K_{ATP}-GOF mice correlates with an early improvement in insulin sensitivity, which precedes the separation in blood glucose. To our surprise, all K_{ATP}-GOF mice fed with HFD demonstrate resistance to HFD-induced obesity, results that correlate with protection from HFD-induced obesity in other insulin secretory-deficient mouse models [18,19]. It has been recently demonstrated that there is an upregulation of 244 genes and downregulation of 109 genes in visceral adipose tissue of wild-type mice that later developed severe insulin resistance compared to those that showed mild insulin resistance even before exposure to HFD[20]. This possibility cannot be ruled out in our study, although un-induced K_{ATP}-GOF mice did not show any basal differences in insulin sensitivity. Mice with adipocyte specific insulin receptor knockout are also protected against diet-induced obesity, hyperinsulinemia, dyslipidemia and insulin resistance[21,22]. Together, these results suggest that both insulin secretion and action may play a critical role in resistance to HFD-induced obesity. Reduced insulin secretion and decreased body fat mass was shown in obese human subjects pharmacologically treated with octreotide (somatostatin analogue) or diazoxide (K_{ATP} channel opener)[23,24]. Diazoxide treatment promotes similar effects as having K_{ATP}-GOF

mutations where K_{ATP} channels are maintained in the open state and therefore insulin secretion is prevented[25–28].

Is food intake and whole-body fat mass the main factors involved in HFD-induced diabetes remission?

Body weight reflects a balance between food intake and energy consumption; however, dietary recommendations for blood glucose control and their influences in the development and progression of diabetes remain controversial. We demonstrate here that in contrast to K_{ATP}-GOF-NR, K_{ATP}-GOF-R mice exhibit efficient energy control with normal food intake and activity, and therefore better glucose control. We and others have demonstrated that partial or complete suppression of β-cell K_{ATP} channels in mice induces insulin secretion leading to improved glucose tolerance[29–33]. However, these mice become glucose intolerant and under-secrete insulin when fed a HFD[34]. In K_{ATP} knockout mice, the decrease in body weight is associated with depletion of subcutaneous, abdominal and retroperitoneal fat mass, but not visceral fat[35], suggesting an altered balance between energy availability and consumption induced by decreased K_{ATP} activity. Similar to the findings observed in ob/ob mice exposed to ketogenic diet[36], K_{ATP}-GOF-R mice maintain adipose tissue and nutrient balance, without increases in plasma lipids. A recent report in a large cohort of patients that were followed for 14 years demonstrated that high-fat dairy products reduce the risk of developing type-2 diabetes[37]. The conclusions in this study may correlate with our results that HFD could prevent loss of insulin content and β-cell mass in K_{ATP}-GOF-R mice. Similarly, inhibition of diabetes progression was found in a rat model of type-2 diabetes fed a HFD containing 62% fat[38]. The increase in total liver glycogen content in K_{ATP}-GOF-R mice may account for the decrease in food intake and reversion of hyperglycemia, as this phenomenon has been reported in other diabetic mouse models[39]. Together, these results suggest that HFD might be protective in certain forms of diabetes. Moreover, the observed resistance to HFD-induced obesity in K_{ATP}-knockout[35] or K_{ATP}-GOF (this manuscript) provides a basis for potential anti-obesity treatment involving altered K_{ATP} channels.

What is the underlying mechanism of protection of diabetes by fat?

In humans, the effect of HFD on diabetes has conflicting reports with no clear understanding of the underlying mechanisms. HFD is known to accelerate the onset and severity of diabetes in some spontaneously occurring diabetes models[40]. It has been proposed that glucotoxic conditions promote internalization of K_{ATP} channels leading to a decrease in the membrane hyperpolarized state, thereby inducing insulin secretion[41]. Pharmacological inhibition of large conductance K^+-channels leads to higher action potentials in HFD, increased Ca^{+2} currents and insulin secretion[42,43]. ChD fed K_{ATP}-GOF mice showed loss of β-cell identity and dedifferentiation[7] similar to the dedifferentiation observed in other models[44,45]. However, the decrease in insulin content and loss of β-cell mass is prevented in HFD fed K_{ATP}-GOF-R mice, suggesting that limiting β-cell insulin secretory response protects from secondary loss of insulin content and β-cell mass.

Collins and colleagues[46] demonstrated that whereas short periods of HFD enhances glucose-stimulated insulin secretion, long-term results in its decrease. These results were not associated with changes in β-cell electrical activity or intracellular [Ca^{2+}] but involved a

disruption of the tight association between L-type Ca^{2+} channels and the Ca^{2+} sensor for exocytosis[46]. Importantly, in our model, reduced insulin secretion by persistently low intracellular $[Ca^{2+}]$[47] was achieved by expression of a K_{ATP}-GOF mutation in mice[6]. HFD fed K_{ATP}-GOF-R mice demonstrate improved insulin sensitivity, and increased plasma insulin and GLP1 concentrations. GLP1 is known to regulate glucose and energy homeostasis in mice and humans[48,49]. Increased GLP-1 in K_{ATP}-GOF-R mice could explain the increase in plasma insulin, decrease in food intake and improved insulin sensitivity. GLP1 can induce insulin secretion in a K_{ATP}- and Ca^{+2}-independent manner[25,26] and its action is preserved in humans with K_{ATP}-GOF mutations[27], which correlates with the effects seen in our mouse model. FFA can also increase insulin secretion independently of K_{ATP} and Ca^{+2} influxes through L-type calcium channels[28]. However, this effect involves Ca^{+2} influxes through nifedipine-insensitive Ca^{+2}-channels and Ca^{+2}-release from intracellular endoplasmic reticulum stores[50,51]. Control mice fed HFD for 12 weeks become obese, hyperinsulinemic, insulin resistant and glucose intolerant by increasing glucose-induced Ca^{2+}-signaling and cell capacitance, without changing glucose-dependent K_{ATP} activity, slope conductance or plasma membrane potential[52]. FFA can also increase L-type Ca^{+2} channel activity and thereby insulin secretion[53,54], suggesting a HFD effect downstream of K_{ATP}. In addition, vitamin D has a beneficial role in pancreatic β-cell function[55] as well as hepatic lipid and glucose metabolism[56] by increasing intracellular Ca^{+2} in insulin resistant states. Notably, a recent report demonstrated that pharmacological potentiation of vitamin D receptor (VDR) signaling partially restores β-cell function and glucose homeostasis in T2D mouse models[57]. Thus, we cannot exclude the possibility that the changes in metabolic variables and insulin sensitivity observed in K_{ATP}-GOF-R mice are promoted by differential vitamin D and calcium handling. Together, these results suggest that intermediate factors other than glucose metabolism could increase $[Ca^{2+}]_i$ and promote insulin secretion in K_{ATP}-GOF-R mice.

ACKNOWLEDGMENTS

This work was supported by National Institutes of Health grant DK098584 to M.S.R and DK 104735 to B.N.F. The funders had no role in study design, data collection and analysis, decision to publish, or preparation of the manuscript. We thank the Diabetes Models Phenotyping and Morphometric and Metabolic Analysis cores, as part of Diabetes Research Center at Washington University in St Louis for processing samples.

List of Abbreviations

K_{ATP}	ATP-sensitive K^+ channel
GOF	Gain-of-function
HFD	High-fat-diet
ChD	Chow-diet
Ctrl	Contro
K_{ATP}-GOF-NR	K_{ATP} channel gain-of-function non-remitter
K_{ATP}-GOF-R	K_{ATP} channel gain-of-function remitter

GLP1	Glucagon-like peptide-1
NDM	Neonatal Diabetes Mellitus
GTT	Glucose tolerance test
ITT	Insulin tolerance test
DEXA	Dual-energy X-ray absorptiometry
MRI	Magnetic resonance imaging
BMD	Bone mass density
RER	Respiratory exchange ratio

REFERENCES

1. Prentki M, Nolan CJ. Islet beta cell failure in type 2 diabetes. J Clin Invest. 2006;116(7):1802–1812. [PubMed: 16823478]
2. Nolan CJ, Damm P, Prentki M. Type 2 diabetes across generations: from pathophysiology to prevention and management. Lancet (London, England). 2011;378(9786):169–181.
3. Muoio DM, Newgard CB. Mechanisms of disease:Molecular and metabolic mechanisms of insulin resistance and beta-cell failure in type 2 diabetes. Nat Rev Mol Cell Biol. 2008;9(3):193–205. [PubMed: 18200017]
4. Gloyn AL, Pearson ER, Antcliff JF, et al. Activating Mutations in the Gene Encoding the ATP-Sensitive Potassium-Channel Subunit Kir6.2 and Permanent Neonatal Diabetes. N Engl J Med. 2004;350(18):1838–1849. [PubMed: 15115830]
5. Koster JC, Remedi MS, Masia R, Patton B, Tong A, Nichols CG. Expression of ATP-insensitive KATP channels in pancreatic beta-cells underlies a spectrum of diabetic phenotypes. Diabetes. 2006;55(11):2957–2964. [PubMed: 17065331]
6. Remedi MS, Kurata HT, Scott A, et al. Secondary consequences of beta cell inexcitability: identification and prevention in a murine model of K(ATP)-induced neonatal diabetes mellitus. Cell Metab. 2009;9(2):140–151. [PubMed: 19187772]
7. Wang Z, York NW, Nichols CG, Remedi MS. Pancreatic beta cell dedifferentiation in diabetes and redifferentiation following insulin therapy. Cell Metab. 2014;19(5):872–882. [PubMed: 24746806]
8. Cnop M, Welsh N, Jonas JC, Jorns A, Lenzen S, Eizirik DL. Mechanisms of pancreatic beta-cell death in type 1 and type 2 diabetes: many differences, few similarities. Diabetes. 2005;54 Suppl 2:S97–107. [PubMed: 16306347]
9. Del Prato S, Bianchi C, Marchetti P. beta-cell function and anti-diabetic pharmacotherapy. Diabetes Metab Res Rev. 2007;23(7):518–527. [PubMed: 17883249]
10. Sakuraba H, Mizukami H, Yagihashi N, Wada R, Hanyu C, Yagihashi S. Reduced beta-cell mass and expression of oxidative stress-related DNA damage in the islet of Japanese Type II diabetic patients. Diabetologia. 2002;45(1):85–96. [PubMed: 11845227]
11. Poitout V, Amyot J, Semache M, Zarrouki B, Hagman D, Fontes G. Glucolipotoxicity of the pancreatic beta cell. Biochimica et biophysica acta. 2010;1801(3):289–298. [PubMed: 19715772]
12. Brommage R Validation and calibration of DEXA body composition in mice. American journal of physiology Endocrinology and metabolism. 2003;285(3):E454–459. [PubMed: 12759224]
13. Remedi MS, Agapova SE, Vyas AK, Hruz PW, Nichols CG. Acute Sulfonylurea Therapy at Disease Onset Can Cause Permanent Remission of KATP-Induced Diabetes. Diabetes. 2011.
14. Halban PA, Polonsky KS, Bowden DW, et al. beta-cell failure in type 2 diabetes: postulated mechanisms and prospects for prevention and treatment. Diabetes Care. 2014;37(6):1751–1758. [PubMed: 24812433]

15. Weir GC, Bonner-Weir S. Islet beta cell mass in diabetes and how it relates to function, birth, and death. Annals of the New York Academy of Sciences. 2013;1281:92–105. [PubMed: 23363033]
16. Robertson RP, Harmon J, Tran PO, Poitout V. Beta-cell glucose toxicity, lipotoxicity, and chronic oxidative stress in type 2 diabetes. Diabetes. 2004;53 Suppl 1:S119–124. [PubMed: 14749276]
17. Templeman NM, Skovso S, Page MM, Lim GE, Johnson JD. A causal role for hyperinsulinemia in obesity. J Endocrinol. 2017;232(3):R173–R183. [PubMed: 28052999]
18. Mehran AE, Templeman NM, Brigidi GS, et al. Hyperinsulinemia drives diet-induced obesity independently of brain insulin production. Cell Metab. 2012;16(6):723–737. [PubMed: 23217255]
19. Vetterli L, Carobbio S, Frigerio F, Karaca M, Maechler P. The Amplifying Pathway of the beta-Cell Contributes to Diet-induced Obesity. The Journal of biological chemistry. 2016;291(25): 13063–13075. [PubMed: 27137930]
20. Chen K, Jih A, Osborn O, et al. Distinct gene signatures predict insulin resistance in young mice with high fat diet-induced obesity. Physiol Genomics. 2018;50(3):144–157. [PubMed: 29341863]
21. Bluher M, Michael MD, Peroni OD, et al. Adipose tissue selective insulin receptor knockout protects against obesity and obesity-related glucose intolerance. Developmental cell. 2002;3(1): 25–38. [PubMed: 12110165]
22. Robertson RP, Lanz KJ, Sutherland DE, Seaquist ER. Relationship between diabetes and obesity 9 to 18 years after hemipancreatectomy and transplantation in donors and recipients. Transplantation. 2002;73(5):736–741. [PubMed: 11907419]
23. Lustig RH, Greenway F, Velasquez-Mieyer P, et al. A multicenter, randomized, double-blind, placebo-controlled, dose-finding trial of a long-acting formulation of octreotide in promoting weight loss in obese adults with insulin hypersecretion. Int J Obes (Lond). 2006;30(2):331–341. [PubMed: 16158082]
24. van Boekel G, Loves S, van Sorge A, Ruinemans-Koerts J, Rijnders T, de Boer H. Weight loss in obese men by caloric restriction and high-dose diazoxide-mediated insulin suppression. Diabetes Obes Metab. 2008;10(12):1195–1203. [PubMed: 18476985]
25. Yamada S, Komatsu M, Aizawa T, et al. Time-dependent potentiation of the beta-cell is a Ca2+-independent phenomenon. J Endocrinol. 2002;172(2):345–354. [PubMed: 11834452]
26. Yajima H, Komatsu M, Schermerhorn T, et al. cAMP enhances insulin secretion by an action on the ATP-sensitive K+ channel-independent pathway of glucose signaling in rat pancreatic islets. Diabetes. 1999;48(5):1006–1012. [PubMed: 10331404]
27. Bourron O, Chebbi F, Halbron M, et al. Incretin effect of glucagon-like peptide 1 receptor agonist is preserved in presence of ABCC8/SUR1 mutation in beta-cell. Diabetes Care. 2012;35(11):e76. [PubMed: 23093687]
28. Komatsu M, Yajima H, Yamada S, et al. Augmentation of Ca2+-stimulated insulin release by glucose and long-chain fatty acids in rat pancreatic islets: free fatty acids mimic ATP-sensitive K+ channel-independent insulinotropic action of glucose. Diabetes. 1999;48(8):1543–1549. [PubMed: 10426371]
29. Koster JC, Remedi MS, Flagg TP, et al. Hyperinsulinism induced by targeted suppression of beta cell KATP channels. Proc Natl Acad Sci U S A. 2002;99(26):16992–16997. [PubMed: 12486236]
30. Miki T, Tashiro F, Iwanaga T, et al. Abnormalities of pancreatic islets by targeted expression of a dominant-negative KATP channel. Proc Natl Acad Sci U S A. 1997;94(22):11969–11973. [PubMed: 9342346]
31. Miki T, Nagashima K, Tashiro F, et al. Defective insulin secretion and enhanced insulin action in KATP channel- deficient mice. Proc Natl Acad Sci U S A. 1998;95(18):10402–10406. [PubMed: 9724715]
32. Seghers V, Nakazaki M, DeMayo F, Aguilar-Bryan L, Bryan J. Sur1 knockout mice. A model for K(ATP) channel-independent regulation of insulin secretion. The Journal of biological chemistry. 2000;275(13):9270–9277. [PubMed: 10734066]
33. Babenko AP, Bryan J. SUR-dependent modulation of KATP channels by an N-terminal KIR6.2 peptide. Defining intersubunit gating interactions. The Journal of biological chemistry. 2002;277(46):43997–44004. [PubMed: 12213829]

34. Remedi MS, Koster JC, Markova K, et al. Diet-Induced Glucose Intolerance in Mice With Decreased {beta}-Cell ATP-Sensitive K+ Channels. Diabetes. 2004;53(12):3159–3167. [PubMed: 15561946]
35. Park YB, Choi YJ, Park SY, et al. ATP-Sensitive Potassium Channel-Deficient Mice Show Hyperphagia but Are Resistant to Obesity. Diabetes Metab J. 2011;35(3):219–225. [PubMed: 21785741]
36. Badman MK, Kennedy AR, Adams AC, Pissios P, Maratos-Flier E. A very low carbohydrate ketogenic diet improves glucose tolerance in ob/ob mice independently of weight loss. American journal of physiology Endocrinology and metabolism. 2009;297(5):E1197–1204. [PubMed: 19738035]
37. Ericson U, Hellstrand S, Brunkwall L, et al. Food sources of fat may clarify the inconsistent role of dietary fat intake for incidence of type 2 diabetes. Am J Clin Nutr. 2015;101(5):1065–1080. [PubMed: 25832335]
38. Ishii Y, Ohta T, Sasase T, et al. A high-fat diet inhibits the progression of diabetes mellitus in type 2 diabetic rats. Nutr Res. 2010;30(7):483–491. [PubMed: 20797481]
39. Lopez-Soldado I, Zafra D, Duran J, Adrover A, Calbo J, Guinovart JJ. Liver glycogen reduces food intake and attenuates obesity in a high-fat diet-fed mouse model. Diabetes. 2015;64(3):796–807. [PubMed: 25277398]
40. Corsetti JP, Sparks JD, Peterson RG, Smith RL, Sparks CE. Effect of dietary fat on the development of non-insulin dependent diabetes mellitus in obese Zucker diabetic fatty male and female rats. Atherosclerosis. 2000;148(2):231–241. [PubMed: 10657558]
41. Han YE, Chun JN, Kwon MJ, et al. Endocytosis of KATP Channels Drives Glucose-Stimulated Excitation of Pancreatic beta Cells. Cell Rep. 2018;22(2):471–481. [PubMed: 29320741]
42. Jacobson DA, Mendez F, Thompson M, Torres J, Cochet O, Philipson LH. Calcium-activated and voltage-gated potassium channels of the pancreatic islet impart distinct and complementary roles during secretagogue induced electrical responses. J Physiol. 2010;588(Pt 18):3525–3537. [PubMed: 20643768]
43. Braun M, Ramracheya R, Bengtsson M, et al. Voltage-gated ion channels in human pancreatic beta-cells: electrophysiological characterization and role in insulin secretion. Diabetes. 2008;57(6):1618–1628. [PubMed: 18390794]
44. Laybutt DR, Glandt M, Xu G, et al. Critical reduction in beta-cell mass results in two distinct outcomes over time. Adaptation with impaired glucose tolerance or decompensated diabetes. The Journal of biological chemistry. 2003;278(5):2997–3005. [PubMed: 12438314]
45. Jonas JC, Sharma A, Hasenkamp W, et al. Chronic hyperglycemia triggers loss of pancreatic beta cell differentiation in an animal model of diabetes. The Journal of biological chemistry. 1999;274(20):14112–14121. [PubMed: 10318828]
46. Collins SC, Hoppa MB, Walker JN, et al. Progression of diet-induced diabetes in C57BL6J mice involves functional dissociation of Ca2(+) channels from secretory vesicles. Diabetes. 2010;59(5): 1192–1201. [PubMed: 20150285]
47. Benninger RK, Remedi MS, Head WS, Ustione A, Piston DW, Nichols CG. Defects in beta cell Ca(2)+ signalling, glucose metabolism and insulin secretion in a murine model of K(ATP) channel-induced neonatal diabetes mellitus. Diabetologia. 2011;54(5):1087–1097. [PubMed: 21271337]
48. MacDonald PE, El-Kholy W, Riedel MJ, Salapatek AM, Light PE, Wheeler MB. The multiple actions of GLP-1 on the process of glucose-stimulated insulin secretion. Diabetes. 2002;51 Suppl 3:S434–442. [PubMed: 12475787]
49. Cernea S, Raz I. Therapy in the early stage: incretins. Diabetes Care. 2011;34 Suppl 2:S264–271. [PubMed: 21525466]
50. Itoh Y, Kawamata Y, Harada M, et al. Free fatty acids regulate insulin secretion from pancreatic beta cells through GPR40. Nature. 2003;422(6928):173–176. [PubMed: 12629551]
51. Nolan CJ, Madiraju MS, Delghingaro-Augusto V, Peyot ML, Prentki M. Fatty acid signaling in the beta-cell and insulin secretion. Diabetes. 2006;55 Suppl 2:S16–23. [PubMed: 17130640]

52. Gonzalez A, Merino B, Marroqui L, et al. Insulin hypersecretion in islets from diet-induced hyperinsulinemic obese female mice is associated with several functional adaptations in individual beta-cells. Endocrinology. 2013;154(10):3515–3524. [PubMed: 23867214]

53. Olofsson CS, Salehi A, Holm C, Rorsman P. Palmitate increases L-type Ca2+ currents and the size of the readily releasable granule pool in mouse pancreatic beta-cells. J Physiol. 2004;557(Pt 3): 935–948. [PubMed: 15090611]

54. Tian Y, Corkey RF, Yaney GC, Goforth PB, Satin LS, Moitoso de Vargas L. Differential modulation of L-type calcium channel subunits by oleate. American journal of physiology Endocrinology and metabolism. 2008;294(6):E1178–1186. [PubMed: 18430963]

55. Wolden-Kirk H, Rondas D, Bugliani M, et al. Discovery of molecular pathways mediating 1,25-dihydroxyvitamin D3 protection against cytokine-induced inflammation and damage of human and male mouse islets of Langerhans. Endocrinology. 2014;155(3):736–747. [PubMed: 24424042]

56. Cheng S, So WY, Zhang D, Cheng Q, Boucher BJ, Leung PS. Calcitriol Reduces Hepatic Triglyceride Accumulation and Glucose Output Through Ca2+/CaMKKβ/AMPK Activation Under Insulin-Resistant Conditions in Type 2 Diabetes Mellitus. Curr Mol Med. 2016;16(8):747–758. [PubMed: 27658467]

57. Wei Z, Yoshihara E, He N, et al. Vitamin D Switches BAF Complexes to Protect beta Cells. Cell. 2018;173(5):1135–1149 e1115. [PubMed: 29754817]

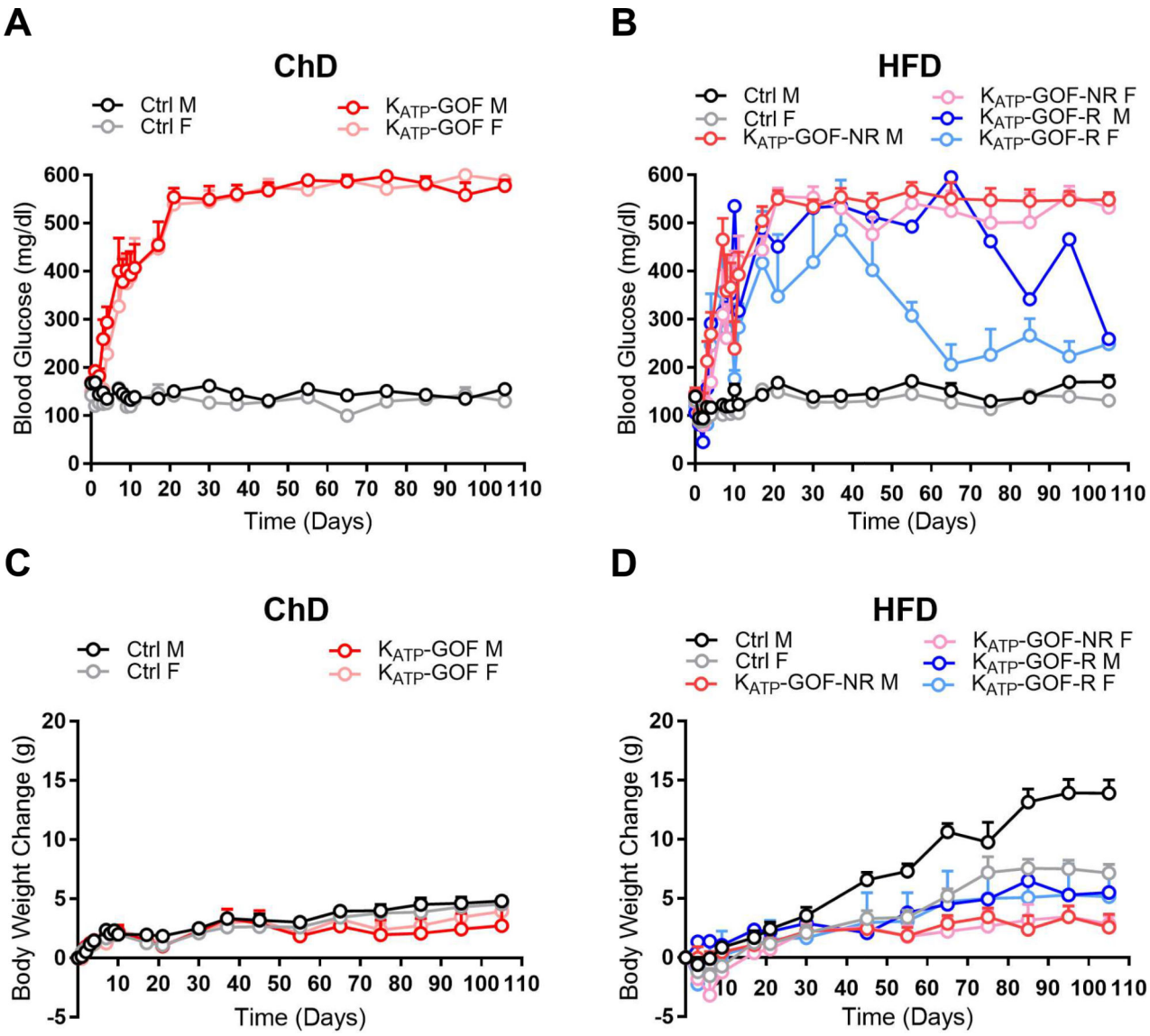

Figure 1.

Fed blood glucose over time after tamoxifen injection in animals exposed to chow diet, ChD **(A)** and high-fat-diet, HFD **(B)**. Body weight change in ChD **(C)** and HFD **(D)** fed mice. Black and grey symbols represent control males and females, respectively; either in ChD (A,C) or HFD (B,D), Red and pink symbols represent K_{ATP}-GOF-NR male and female mice, respectively, either in ChD (A,C) or HFD (B,D); and blue and light blue symbols represent K_{ATP}-GOF-R male and female mice, respectively, either in ChD (A,C) or HFD (B,D). Values represent mean+s.e.m, n=4–10 mice.

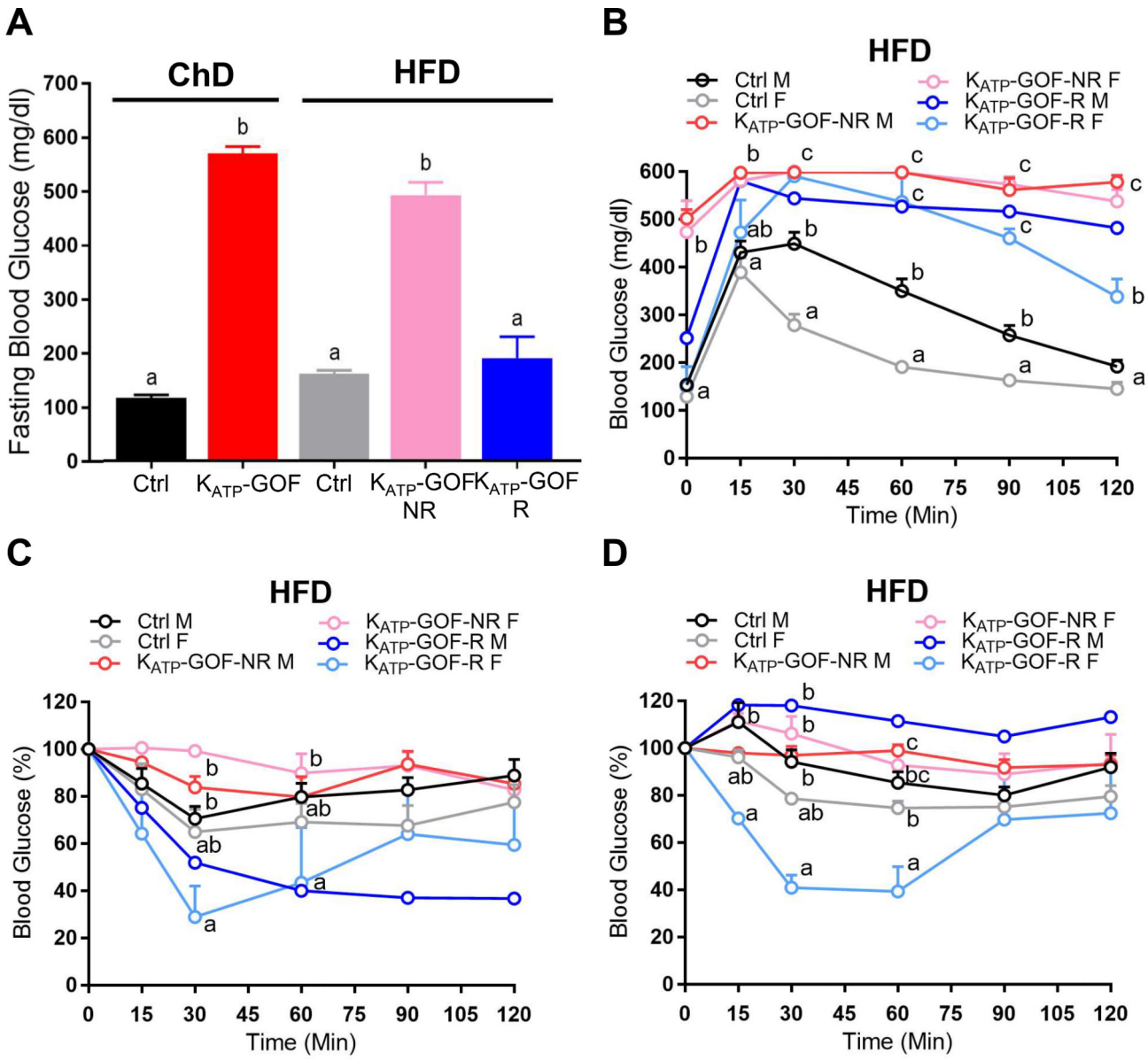

Figure 2.

Fasting blood glucose **(A)** and glucose tolerance test **(B)** in ChD and HFD fed mice at 100 days post-tamoxifen. Insulin tolerance test after 21 days **(C)** and 120 days **(D)** post-tamoxifen injection. Values represent mean + s.e.m; n=4–10 mice. Different letters indicate significant differences between groups in blood glucose from repeated-measures ANOVA (significance $p < 0.05$). Black and grey symbols represent control males and females, respectively, fed with ChD (A,C) or HFD (B,D), Red and pink symbols represent K_{ATP}-GOF-NR male and female mice, respectively, fed with ChD (A,C) or HFD (B,D). Blue and light blue symbols represent K_{ATP}-GOF-R male and female mice, respectively, fed with ChD (A,C) or HFD (B,D).

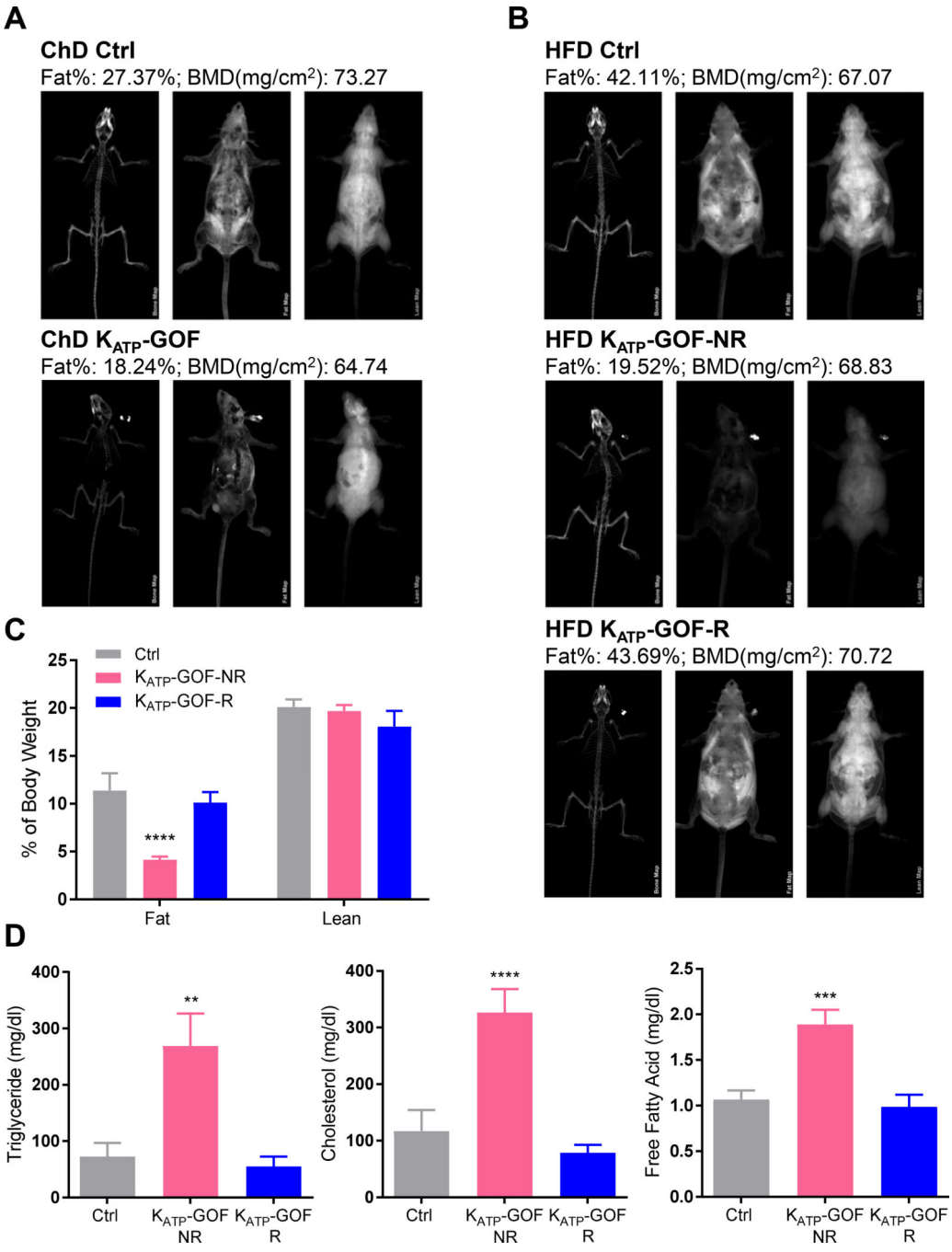

Figure 3.

Whole body composition analysis using DEXA in ChD **(A)** and HFD **(B)** fed mice. Pictures of bone map, fat map, and lean map on each mouse were taken. The whole body percentage of fat (Fat%) and amount of minerals within bone (BMD) are provided on top of each mouse picture. **(C)** Analysis of percentage body fat and lean mass from MRI on HFD fed control (grey), K_{ATP}-GOF-NR (pink) and K_{ATP}-GOF-R (blue) mice. Values represent mean + s.e.m; ****p< 0.0001; n=3–10. **(D)** Plasma lipids (triglyceride, cholesterol and free fatty acids) from HFD fed control (grey), K_{ATP}-GOF-NR (pink) and K_{ATP}-GOF-R (blue) mice. Values

represent mean+s.e.m; significance *p <0.05; **p <0.01; ***p <0.001; ****p <0.0001; n=4–10 mice.

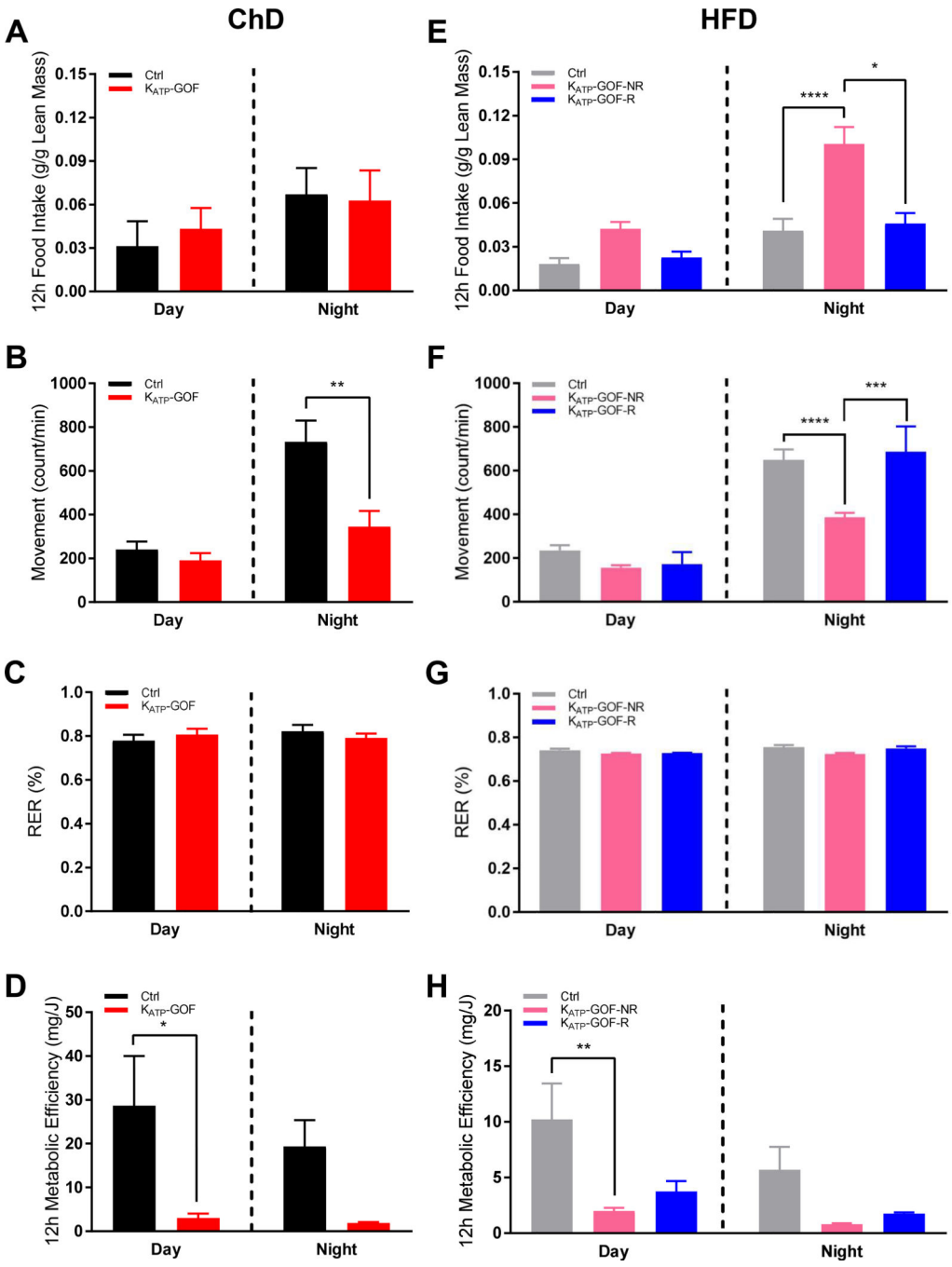

Figure 4.

Metabolic analysis for ChD fed mice: food intake **(A)**, physical activity **(B)**, RER **(C)** and metabolic efficiency **(D)** within 12 hours during the day and at night for control (black) and K_{ATP}-GOF (red). Metabolic analysis for HFD fed mice: food intake **(E)**, physical activity **(F)**, RER **(G)** and metabolic efficiency **(H)** within 12 hours during day and night for control (grey), K_{ATP}-GOF-NR (pink) and K_{ATP}-GOF-R (blue). Values represent mean+s.e.m, significance * p<0.05; ** p<0.01; *** p<0.001; **** p<0.0001; n=4–10 mice.

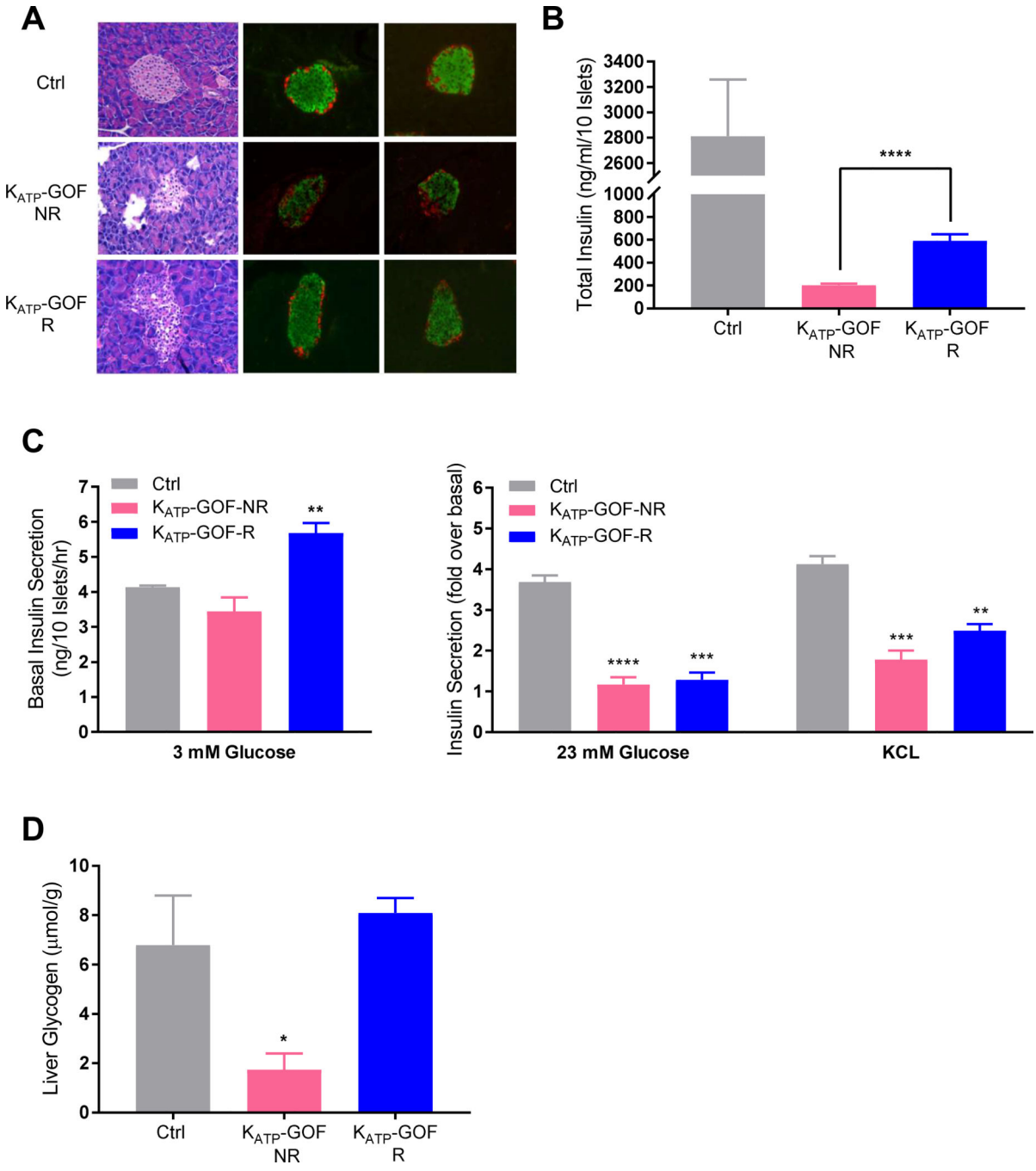

Figure 5.

(A) Representative images of pancreatic paraffin sections stained for hematoxylin-eosin (H&E) (left panel) and double-stained for insulin (green) /glucagon (red) (middle and right panels). **(B)** Total insulin content per 10 islets **(C)** Basal insulin secretion at non-stimulatory (3mM) glucose (left), and fold over basal glucose (23mM) and KCl stimulated insulin secretion (right) per 10 islets in one hour. **(D)** Liver glycogen content per gram of tissue. HFD fed control (grey), K_{ATP}-GOF-NR (pink) and K_{ATP}-GOF-R (blue) mice. Values

represent mean+s.e.m; significance *p<0.05; **p<0.01; ***p<0.001; ****p<0.0001; n=3–10 mice.

Table 1.

Plasma hormone measurements.

	HFD 22 Days			HFD 110 Days		
	Ctrl	**Kir6.2-GOF-NR**	**Kir6.2-GOF-R**	**Ctrl**	**Kir6.2-GOF-NR**	**Kir6.2-GOF-R**
Insulin (pg/ml	528.9±172.2	291.2±80.6	213.3±48.4	694.0±159.2	63.9±4.7*	503.4±182.7
Glucagon (pg/ml)	6.4±1.1	8.4±2.1	10.6±0.4*	9.9±1.6	9.5±0.4	12.6±1.9
Leptin (pg/ml)	897±327	549.0±160.8	554.9±345.6	2813.0±621.5	310.7±121.4*	2321.0±1115.0
GLP-1 (pg/ml)	3.2±1.0	7.0±2.4	7.2±1.3	4.2±0.7	6.9±1.0	21.3±3.8*

Table 1 shows plasma insulin, glucagon, leptin and GLP1 concentrations in K_{ATP}-GOF-R, K_{ATP}-GOF-NR and control mice fed with HFD for 22 and 110 days. Values represent mean+s.e.m, significance

*$p<0.05$ n=3–7 mice/group.